Journal of Computational and Applied Mechanics, Vol. 12. No. 2. (2017), pp. 85–98
DOI: 10.32973/jcam.2017.006

ASPECTS ON MODELING THE MECHANICAL BEHAVIOR OF ALUMINUM ALLOYS WITH DIFFERENT HEAT TREATMENTS

Camelia Cerbu and Horatio Teodorescu-Draghicescu
Faculty of Mechanical Engineering, Transilvania University of Braşov
B-dul Eroilor 29, RO-500036, Braşov, ROMANIA
cerbu@unitbv.ro,draghicescu.teodorescu@unitbv.ro

[Received: April 25, 2017; Accepted: September 14, 2017]

Abstract. Mechanical characteristics of two kinds of the EN AW–6060 aluminum alloys were measured in tensile and three-point bending tests. Although there is a standard [20] that indicates the mechanical properties of the aluminum alloys used to manufacture different kinds of profiles, the main purpose of this paper is to compare the accuracy of the mechanical properties of the commercial aluminum alloy EN AW–6060 used to manufacture box profiles in T4 or T6 heat treatment conditions. It is shown that the maximum values $\sigma_{\max}$ of the tensile and flexural stresses – these are denoted by $\sigma_{\max}$ – are 41.55% and 75.12% greater for the EN AW–6060–T6 aluminum alloy than those for the EN AW–6060–T4 aluminum alloy. There are small differences concerning the modulus of elasticity E recorded: 7.52% for the case of Young's modulus E in the tensile test; 5.34% for the modulus of elasticity in the three-point bending test. Both kinds of aluminum alloys have elastic-plastic behavior in tensile test. Theoretical concepts regarding the modeling of the nonlinear behavior of the elastic-plastic materials in the plastic range of the material are considered in order to simulate the behavior of the aluminum alloys in the tensile tests by using finite element analysis (FEA). Finally, we should remark that the $(\sigma - \varepsilon)$ stress-strain curves obtained in the numerical modeling match with those experimentally obtained for each aluminum alloy we have analyzed. Thus the input parameters for FEA (Young's modulus E, the true stresses and strains belonging to the plastic range) for each type of aluminum alloy tested may be used in the case of any structural element made of such alloys.

Keywords: aluminum alloy, tensile test, bending test, heat treatment

1. Nomenclature

Latin symbols

A_o	initial area of the cross-section of the tensile specimen,
A	instantaneous area of the cross-section of the tensile specimen at a certain time of loading in the plastic range
b, h	cross-sectional dimensions of the tensile and flexural specimens,
$_b$, $_t$	these subscripts indicate that the quantity considered was measured in the bending or tensile tests,

CV	coefficient of variation (or relative standard deviation) which is a standardized measure of dispersion; it is the ratio between Stdev and the average value of a set of values, expressed in percentage,
l_0, l	initial active length of the tensile specimen and the length of the specimen corresponding to the tensile force F,
E	modulus of elasticity (Young's modulus),
F	tensile force in the tensile test / external force in the bending test,
p	intensity of the distributed forces acting on the free end of the tensile specimen in FEA,
Stdev	standard deviation of a data set,
$T4, T6$	heat treatment conditions of the aluminum alloy
V_0, V	volume of the specimen at the beginning of the tensile test and at time t,
W	work done until maximum load is reached.

Greek symbols

$\Delta l_{\max}$	elongation of the tensile specimen at maximum load,
$\varepsilon, \varepsilon_{\log}$	engineering and logarithmic strains,
$\varepsilon_{\max}$	maximum strain,
ε_x	strain on the longitudinal axis Ox of the tensile specimen,
$\sigma_{\max}$	maximum stress,
σ_r	true tensile stress,
σ_x	normal stress on the longitudinal axis Ox of the tensile specimen,
$(\sigma_r - \varepsilon_r)$	true stress strain curve in tensile loading.

2. Introduction

The effects of the microstructure as well as the effects of heat and ageing treatments on the mechanical properties of aluminum alloys are presented in references [1–7]. New aluminum alloys have been developed for automotive applications in the last years. Aluminum alloys exhibit an excellent combination of strength and ductility [8]. Different homogenizing, annealing and aging processes of various aluminum alloys have been also investigated [9–11]. Hardness, yield strength and ultimate tensile strength of the AA6063 aluminum alloy after two-stage solution treatment were significantly increased, while elongation to failure remained unchanged [12]. Porosity evaluation on the fracture surfaces of AlSi10MnMg(Fe) secondary alloys was investigated showing an increasing of the porosity at these surfaces [13]. Fatigue and mechanical behaviors at high temperatures during welding of different kinds of aluminum alloys are presented in [14–16]. The influence of the composition of the aluminum alloy and the heat treatment on their mechanical properties resulted in, for instance, a high rate change in hardness during quick cooling [17, 18]. The effects of the different treatments on the mechanical properties and the microstructure of Al-Zn-Mg(-Cu) based aluminum alloys are also discussed in [19].

The main purpose of the present paper is to show the effects of thermal treatment on the mechanical properties of the EN AW–6060 AlMgSi aluminum alloy using tensile specimens cut from extruded box profiles. The alloy EN AW–6060 AlMgSi is a widely used extrusion alloy. It is recommended for applications such as the following: frame profiles for windows, doors, curtain walls, fences, railings, stairs, frame systems for interior accessories, pneumatic equipment, irrigation pipes and pipes for cooling.

Another goal is to define the input parameters for the finite element analysis (FEA) by using the experimental results in order to model the nonlinear behavior of the aluminum alloy for any structure and/or any structural element made of such an alloy. For this purpose we compare the stresses and strains in the tensile specimens determined by the finite element method with the values experimentally obtained in the tensile tests. The input material parameters for FEA are: Young's modulus experimentally obtained from the tensile tests in order to model the behavior of the aluminum in the elastic range and the true stress σ_r and true strain ε_r value pairs computed using experimental results in order to properly model the material behavior of the aluminum in the plastic range. A British standard gives the mechanical properties for the extruded rod/bar, tube and profiles made of aluminum alloys [20].

In order to show the effects of the thermal treatment on the EN AW–6060 AlMgSi aluminum alloy, two kinds of this alloy were tested: the EN AW–6060-T4–aluminum alloy in T4 heat treatment condition and the EN AW–6060-T6–aluminum alloy in T6 heat treatment condition. The T4 heat treatment condition corresponds to naturally aged to a stable condition while T6 heat treatment condition corresponds to solution heat treated, quenched and artificially aged [21].

3. Theoretical issues

It is known that aluminum has elastic-plastic behavior under mechanical load. It should, therefore, be taken into account that a decreasing of the cross-section A takes place in the plastic range of loading as the tensile force F increases. In the plastic range, it is customary to define a logarithmic strain $\varepsilon_{\log}$ by the following relationship [22]:

$$\varepsilon_{\log} = \int_{l_0}^{l} \frac{\mathrm{d}l}{l} \tag{1}$$

where l_0 is the initial active length of the tensile specimen and is the length of the specimen corresponding to the tensile force The logarithmic strain (1) is a nonlinear function of the length l. The following relation follows from (1) between the logarithmic strain $\varepsilon_{\log}$ and the engineering strain ε [22]:

$$\varepsilon_{\log} = \ln \frac{l}{l_0} = \ln \frac{l_0 + \Delta l}{l_0} = \ln\left(1 + \varepsilon\right). \tag{2}$$

The stress that corresponds to the logarithmic strain $\varepsilon_{\log}$ is the true tensile stress:

$$\sigma_r = F/A \tag{3}$$

where A is the instantaneous area of the cross-section in the tensile specimen.

In the case of nonlinear material behavior we shall assume that the volume of the tensile specimen remains unchanged:

$$V = V_0, \qquad \Rightarrow \qquad Al = A_0 l_0\,. \tag{4}$$

Hence

$$A = \frac{A_0 \cdot l_0}{l} = \frac{A_0}{\frac{l}{l_0}} = \frac{A_0}{1+\varepsilon}. \tag{5}$$

Substituting (5) into (3), we obtain the following relation between the true stress σ_r and the engineering stress σ [22]:

$$\sigma_r = \frac{F}{A} = \frac{F\,(1+\varepsilon)}{A_0} \qquad \Rightarrow \qquad \sigma_r = \sigma\,(1+\varepsilon)\ . \tag{6}$$

The true stress-strain curve $\sigma_r - \varepsilon_r$ can be drawn by using the true values of the stresses σ_r and logarithmic strains $\varepsilon_{\log}$ computed on the basis of relations (2) and (6).

4. Materials and work method

4.1. **Materials.** In accordance with European Standard SR-EN 573 – 3 / 2010 [24], EN AW–6060 aluminum alloy belongs to the series 6000 of the aluminum alloys AlMgSi (aluminum–magnesium–silicon). Chemical composition of the aluminum alloy EN AW 6060 is: 0.3-0.6% Si; 0.1-0.3% Fe; 0.10% Cu; 0.35-0.60 % Mg; 0.05 % Cr; 0.15% Zn; 0.10 % Ti; 0.05 % other metallic components so as not to exceed 0.15%; the difference is covered by the aluminum [24]. According to [25] the EN AW–6060 aluminum alloy in T4 or T6 heat treatment condition are encoded as: EN AW–6060-T4 or EN AW–6060-T6, respectively.

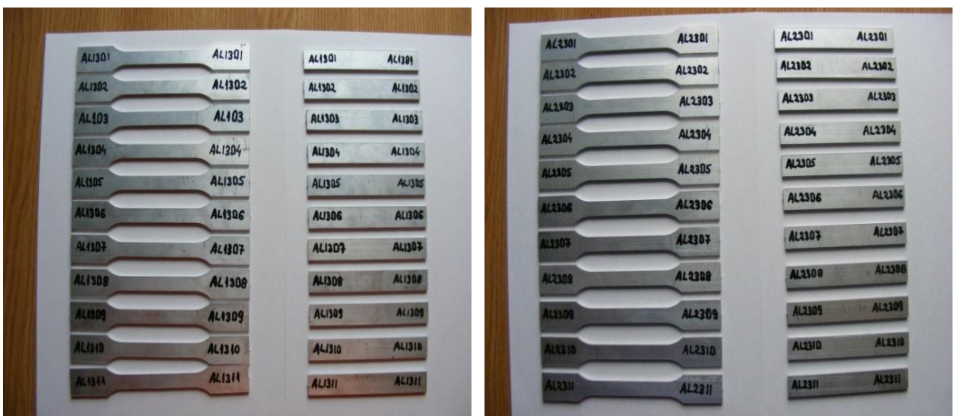

a. b. c. d.

Figure 1. Specimens for testing: a, b - Tensile/flexural specimens made of aluminum alloy EN AW–6060–T4; c, d - Tensile/flexural specimens made of aluminum alloy EN AW–6060–T6

The tensile specimens shown in Figure 1a and c are manufactured according to European Standard EN ISO 6892-1: 2002 [26]. Some dimensions of the tensile specimen are: total length – 150 mm, active length $l_0 = 60$ mm, the width of the active length is $b = 10$ mm, the width of end part that is clamped in the tensile machine is $B = 20$ mm.

The flexural specimens shown in Figure 1b and d have 120 mm in length and the width of the rectangular cross-section is 15 mm. The thickness is 3 mm for both kinds of specimens.

The tensile and flexural specimens are cut from commercial profiles having a box cross-section and made of EN AW–6060 aluminum alloy which was subjected to two different heat treatment conditions (T4 and T6).

4.2. **Work method.**

4.2.1. *Experimental methods.* For the tensile tests we used a tensile machine manufactured by LLOYD Instruments (West Sussex, United Kingdom). Its maximum load capacity is ±50 kN. The speed of loading was 3 mm/min in accordance with the European Standard EN ISO 6892-1: 2002 [26]. An extensometer was used in order to record the elongation of the specimen. The initial span between the marks of the tensile specimen that is the initial active length was equal to 50 mm [26].

A LR5K Plus machine manufactured by LLOYD Instruments (West Sussex, United Kingdom) was used for the three-point bending test. Its maximum load capacity is ±15 kN. The flexural specimen was simply supported at its ends during testing and the span between the supports was equal to 80 mm. The crosshead speed was 15 mm/min.

4.2.2. *Theoretical investigations.* Finite element analysis (FEA) was used to simulate the mechanical behavior of the aluminum tensile specimen in the tensile test. The main objective of FEA was to compare the stress-strain curve obtained for the element located at the middle of the specimen with the experimentally obtained stress-strain curve. Consequently, the graph of the true stress-strain curve ($\sigma_r - \varepsilon_r$) will be the output result presented in Subsection 5.3 Theoretical versus experimental results. If the theoretical curve matches with the experimental one, the input parameters of the material used in FEA can also be used for any structure made of such kinds of aluminum. Another goal of FEA is to compare the maximum theoretical value of the tensile stress $\sigma_{\max}$ obtained from the finite element model (FEM) with the value recorded in the tensile test.

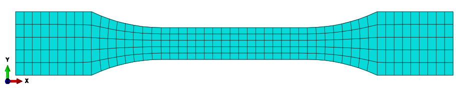

Figure 2. Finite element model (FEM)

Figure 3. Boundary conditions and load applied

The geometrical model for the finite element analysis of the tensile specimen was designed in accordance with the dimensions specified in [26] and also used to manufacture the tensile specimens. The finite element model (FEM) is shown in Figure 2. Four-node plane stress finite elements were applied to numerically model the stress and strain states in the tensile specimen. Figure 3 shows the boundary conditions applied (one end of the specimen is fixed) and the distributed force p exerted on the other end of the tensile specimen.

Two different cases were considered in the finite element analysis concerning the properties of the material assigned to the models of the tensile specimens: 1) properties of the EN AW–6060–T4 aluminum alloy; 2) properties of the EN AW–6060–T6 aluminum alloy.

The material input parameters used in FEA are based both on the experimental results obtained in tensile tests and on the quantities computed by using relations (2) and (6) in order to model the elastic-plastic behavior of the aluminum alloy in each case. Therefore, Young's modulus E experimentally obtained in tensile test was an input data for the finite element analysis to model the material behavior of the aluminum in the elastic range of the stress-strain curve $(\sigma - \varepsilon)$. To model the mechanically behavior in the plastic range of the stress-strain curve $(\sigma - \varepsilon)$, we used the true stress σ_r and true strain ε_r value pairs computed by utilizing relations (2) and (6), respectively. The average stress-strain curves $(\sigma - \varepsilon)$ calculated from the experimentally recorded stress strain curves (see Figure 4) were also considered as input data for each aluminum alloy in order to describe their mechanical behavior in the plastic range.

The value of the Poisson coefficient ν was set at $\nu = 0.33$ for the EN AW–6060 aluminum alloy according to [27].

The dimensions for the geometrical models of the tensile specimens were the same as those of tensile specimens in the tensile tests.

In this way we can compare the stress and strain states obtained from the finite element computations or the experiments for each aluminum alloy.

Finally, the true stress-strain curve $(\sigma_r - \varepsilon_r)$ obtained from finite element analysis FEA analysis, which is based on theoretical concepts presented in Section 2, is compared with the conventional stress-strain curves $(\sigma - \varepsilon)$ recorded in the tensile tests of each aluminum alloy.

5. Results

5.1. **Experimental results.** The stress-strain curves $(\sigma - \varepsilon)$ recorded in tensile tests are shown in Figure 4. Note that after the yield point, the curves $(\sigma - \varepsilon)$ corresponding

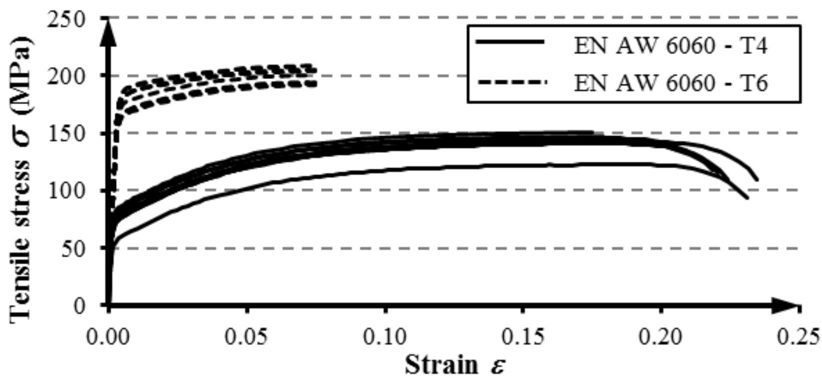

Figure 4. Stress strain curve $(\sigma - \varepsilon)$ recorded in the tensile test

to the EN AW–6060–T4 aluminum alloy are located above the stress strain curves of the EN AW–6060–T6 aluminum alloy. This remark shows that the maximum value of the tensile stress $\sigma_{\max}$ is greater for the EN AW–6060–T6 aluminum alloy than for the EN AW–6060–T4 aluminum alloy. But the maximum axial strain $\varepsilon_{t\ \max}$ recorded at the maximum force $F_{\max}$ is less for the EN AW–6060–T6 aluminum alloy than for the EN AW–6060–T4 aluminum alloy.

Table 1. Mechanical properties for material EN AW–6060–T4 in tensile test

No. of the tensile specimen	Width b (mm)	Thickness h (mm)	Young's modulus E (MPa)	Maximum load (N)	Max. tensile stress $\sigma_{t\max}$ (MPa)	Elongation at max. load $\Delta l_{\max}$ (mm)	Max. strain at max. load $\varepsilon_{t\max}$	Work to max. load W_t (Nmm)
1	10.03	3.00	64637	3689	123	9.307	0.186	30110
2	10.02	3.00	49239	4253	142	8.576	0.172	32164
3	10.04	2.98	60051	4364	146	7.961	0.159	30701
4	10.03	2.97	69708	4233	142	9.855	0.197	37372
5	10.03	2.97	68511	4196	141	9.321	0.186	34841
6	10.04	3.00	41589	4429	147	8.751	0.175	34608
7	10.02	2.98	69443	4277	143	9.874	0.197	37969
8	10.02	3.00	35984	4308	143	9.940	0.199	38553
9	10.02	2.96	66626	4480	151	8.561	0.171	34147
10	10.03	2.96	57231	4195	141	8.632	0.173	31924
Average value	10.03	2.98	58302	4242	142	9.078	0.182	34239
Stdev	0.008	0.017	12164	217	7.36	0.68	0.014	3020
CV	0.08%	0.57%	20.86%	5.12%	5.18%	7.49%	7.69%	8.82%

Table 2. Mechanical properties for material EN AW–6060–T6 in tensile test

No. of the tensile specimen	Width b (mm)	Thickness h (mm)	Young's modulus E (MPa)	Maximum load (N)	Max. tensile stress $\sigma_{t\max}$ (MPa)	Elongation at max. load $\Delta l_{\max}$ (mm)	Max. strain at max. load $\varepsilon_{t\max}$	Work to max. load W_t (Nmm)
1	10.10	3.08	54394	6040	194	3.759	0.075	21198
2	10.12	3.10	50549	6420	205	4.396	0.088	26735
3	10.08	3.06	55699	6443	209	3.842	0.077	23379
4	10.08	3.09	55275	6489	208	4.126	0.083	25376
5	10.08	3.06	52199	6192	201	3.642	0.073	21064
6	10.07	3.07	55148	5988	194	4.650	0.093	26403
7	10.08	3.03	55699	6291	206	4.404	0.088	26244
8	10.04	3.07	58855	6330	205	4.359	0.087	26192
9	10.06	3.09	54329	6028	194	4.280	0.086	24257
10	10.10	3.08	47042	5960	192	4.078	0.083	24365
Average value	10.08	3.07	53919	6218	201	4.154	0.083	24365
Stdev	0.022	0.020	3267	203	6.65	0.32	0.006	2161
CV	0.22%	0.65%	6.06%	3.26%	3.31%	7.70%	7.23%	8.87%

The average values of the mechanical properties recorded in tensile test are shown in Tables 1 and 2 for both tested alloys. The average value of Young's modulus E, which is 58302 MPa for the aluminum alloy EN AW–6060–T4, is greater by 8.13% than that for the aluminum alloy EN AW–6060–T6, which is 5319 MPa. The maximum value of the tensile stress $\sigma_{t\,\max}$ is greater by 41.55% for the EN AW–6060–T6 alloy than for the EN AW–6060–T4 alloy – compare the values 201 MPa and 142 MPa. The maximum strain $\varepsilon_{\max} = 0.182$, which was recorded at the maximum force $F_{\max}$, is greater by 119.28% for EN AW–6060–T4 than for EN AW–6060–T6 since the latter is 0.083. This is the reason why the work done till we reach the maximum load is greater by 40.52% for the EN AW–6060–T4 aluminum alloy than the value recorded for the EN AW–6060–T6 alloy.

Analyzing the coefficients of variation CV corresponding to Young's modulus, we got CV=20.86% which shows more variability of the data set of the EN AW 6060 alloy in T4 heat treatment condition (Table 1). The reason for this is, in all probability, the slipping of some tensile specimens in the grip elements of the tensile machine. The coefficient CV=6.06% is, however, closer to 5% in the case of the EN AW–6060-T6 alloy (Table 2).

As regards the maximum tensile stress, the computed coefficients of variation CV are acceptable because these are equal to 5.18% and 3.31% for the cases of T4 and T6 heat treatment conditions, respectively. This shows less variability of the data set – see again Tables 1 and 2.

The stress-strain curves ($\sigma - \varepsilon$) recorded in the three-point bending test are shown in Figure 5. The curves are shown graphically for the points located at the bottom of the critical cross-section of the flexural specimen (cross-section located at midpoint of the span between supports). The values of the engineering stresses and strains are computed and recorded in a text file, in real-time, by the LR5K Plus machine used for the bending test. Engineering stresses σ and strains ε depend both on the initial dimensions b, h of the flexural specimen and the span between the supports (this is 80 mm) that were entered in the software of the machine before testing.

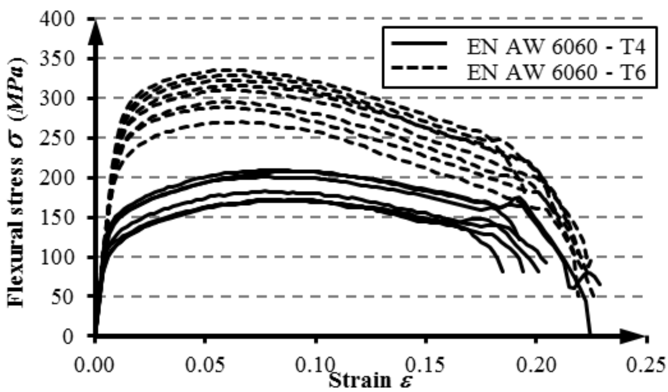

Figure 5. Stress strain curve ($\sigma - \varepsilon$) recorded in the three point bending test

We may observe in Figure 5 that the slopes of the elastic portions of the $(\sigma - \varepsilon)$ curves are greater in the case of the EN AW–6060–T6 aluminum alloy. The $(\sigma - \varepsilon)$ curves for the EN AW–6060–T6 alloy are located above the curves that belong to the other aluminum alloy which is in T4 heat treatment condition. Hence it follows that the modulus of elasticity E in the bending test and the maximum stress $\sigma_{b\,\max}$ – both in the case of EN AWAW–6060–T6 aluminum alloy – are greater than the same values recorded for the other material, i.e., for the EN AW–6060–T4 aluminum alloy (the cross section is the same as before).

Table 3. Mechanical properties for the material EN AW–6060–T4 in the three-point bending test

No. of the flexural speci-men	Width b (mm)	Thick-ness h (mm)	Modulus of elasticity in bending test E (MPa)	Max. force $F_{\max}$ (N)	Max. stress at max. load $\sigma_{b\,\max}$ (MPa)	Max. strain at max. load $\varepsilon_{b\ \max}$	Work to max. load W_b (Nmm)
1	14.99	3.03	24195	210	183	0.080	5072
2	14.97	3.01	25094	235	210	0.081	5832
3	14.98	2.98	28726	191	173	0.078	4535
4	14.96	3.02	26324	228	201	0.075	5228
5	14.97	3.03	24380	196	171	0.092	5431
6	14.97	3.00	24003	193	172	0.092	5431
7	15.03	3.01	23939	236	208	0.091	6581
Average value	14.98	3.01	25237	213	188	0.084	5449
Stdev	0.023	0.018	1751	20	17.55	0.007	640
CV	0.15%	0.60%	6.94%	9.39%	9.34%	8.33%	11.75%

Table 4. Mechanical properties for the material EN AW–6060–T6 in the three-point bending test

No. of the flexural speci-men	Width b (mm)	Thick-ness h (mm)	Modulus of elasticity in bending test E (MPa)	Max. force $F_{\max}$ (N)	Max. stress at max. load $\sigma_{b\,\max}$ (MPa)	Max. strain at max. load $\varepsilon_{b\ \max}$	Work to max. load W_b (Nmm)
1	14.98	3.11	26282	349	289	0.055	5531
2	15.01	3.12	26515	360	296	0.057	5916
3	15.00	3.11	26303	382	316	0.056	6164
4	15.00	3.11	26523	390	323	0.059	6770
5	15.02	3.11	27389	406	336	0.062	7460
6	14.98	3.11	26502	375	311	0.060	5715
7	15.01	3.11	27356	327	270	0.060	5715
8	14.97	3.11	25801	398	330	0.058	6681
Average value	15.00	3.11	26584	373	309	0.058	6345
Stdev	0.018	0.004	540	27	22.39	0.002	637
CV	0.12%	0.13%	2.03%	7.24%	7.25%	3.45%	10.04%

5.2. **Theoretical results.** In the present section it is our aim to determine the stress and strain states in the tensile specimens for those two cases when the material properties are different from each other, i.e., for the EN AW–6060–T4 and EN AW–6060–T6 aluminum alloys. The tensile stress σ_x and axial strain ε_x distributions for the EN AW–6060–T4 aluminum alloy are shown in Figure 6a and b as functions of the plane coordinates of x, y provided that the applied $F = 74196$ N axial force is the maximum value of the axial forces experimentally recorded in the case of those tensile specimens whose $(\sigma - \varepsilon)$ stress-strain curves were considered to determine the behavior of this kind of alloy in the plastic range. It is worth of mentioning that the maximum tensile stress $\sigma_{\max} = 140.1$ MPa (see Figure 6a) obtained from the finite element analysis is approximately equal to the average value 142 MPa obtained from the experiments (Table 1).

In the same manner, Figure 7 shows the distributions of the tensile stresses and strains regarding the case of the other material, i.e., for the EN AW–6060–T6 aluminum alloy. The maximum tensile stress (Figure 7a) obtained from the finite element analysis is again approximately equal to the average value of the experimental results (Table 2).

In Figures 6 and 7, the plots that depicts the un-deformed and deformed shapes of the tensile specimen are overlapped in order to highlight the elongation and the transversal contraction. It has to be noted that the deformation scale factor is equal to 5 in the case of the plots.

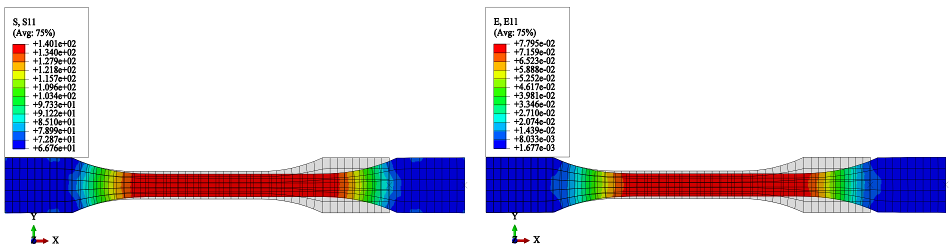

a. b.

Figure 6. FEA results for material properties EN AW–6060–T4 aluminum alloy: a. Stress; b. Strain

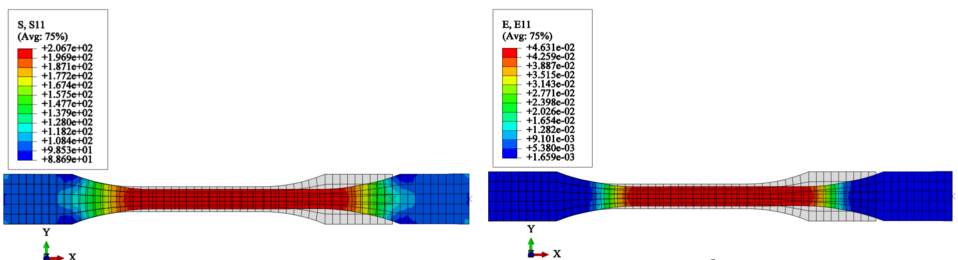

a. b.

Figure 7. FEA results for material properties EN AW–6060–T6 aluminum alloy: a. Stress; b. Strain

It can be mentioned again that although the axial force F applied to the EN AW–6060–T6 aluminum specimen is greater by 47.57% than the axial force applied to EN AW–6060–T4 aluminum specimen, the maximum strain $\varepsilon_{x\,\max} = 4.631 \times 10^{-2}$ recorded for the EN AW–6060–T6 aluminum specimen is smaller by 40.59% than the same quantity for the other aluminum alloy.

5.3. **Theoretical versus experimental results.** In every case we analyzed, the true stress-strain curve $(\sigma_r - \varepsilon_r)$ obtained from the finite element analysis was compared to the stress-strain curve $(\sigma - \varepsilon)$ experimentally determined. The stress-strain curve $(\sigma - \varepsilon)$ was also used to determine the material behavior in the plastic range.

Figure 8a shows comparisons between the stress-strain curve $(\sigma_r - \varepsilon_r)$ of the finite element model and the experimentally recorded stress-strain curve valid for the EN AW–6060–T4 aluminum specimen. A similar comparison is made in Figure 8b for the EN AW–6060–T6 aluminum specimen.

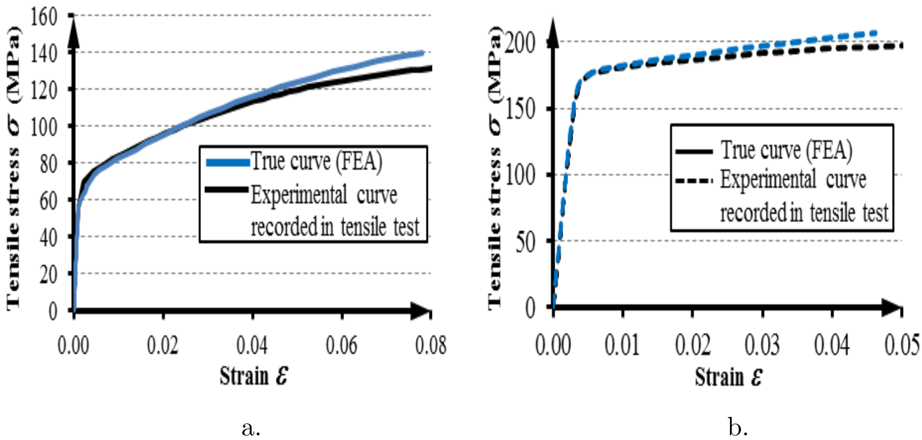

Figure 8. Comparison of the true and experimental stress-strain curves recorded in tensile tests for a. EN AW–6060–T4 aluminum alloy; b. EN AW–6060–T6 aluminum alloy

Figures 8a and 8b show a good fit between both kinds of stress-strain curves. We may therefore come to the conclusion that the material properties of the two aluminum alloys are well-determined for the numerical models of the tensile specimens from the elastic and the plastic point of views as well.

6. Conclusion

We remark that the mechanical properties recorded for the EN AW–6060–T6 aluminum alloy are generally greater than the values recorded for the EN AW–6060–T4 aluminum alloy.

The maximum values of the tensile and flexural stresses $(\sigma_{\max})$ are 41.55% and 75.12% greater in the case of the EN AW–6060–T6 aluminum alloy than in the case of the EN AW–6060–T4 aluminum alloy. With regard to these strength properties, the aluminum EN AW–6060 box profiles in T6 heat treatment condition are recommended instead of the aluminum EN AW–6060 box profiles that are in T4 heat treatment condition in order to manufacture structures and/or structural elements for which high strength is a fundamental requirement.

It is worth of mentioning that the EN AW–6060 aluminum alloy has large plastic deformations in the three-point bending test independently of the heat treatment it was subjected to (Figure 5).

A similar remark can be may made for the EN AW–6060–T4 alloy in the case of the tensile test. The maximum strain $\varepsilon_{\max}$ recorded at the maximum force $F_{\max}$ is more than twice as high (by 119.28%) for the EN AW–6060–T4 alloy ($\varepsilon_{\max} = 0.182$) than for the EN AW–6060–T6 alloy ($\varepsilon_{\max} = 0.083$). These remarks lead to the conclusion that the EN AW–6060-T4 aluminum alloy in T4 heat treatment condition is a ductile material.

The good fit between the $\sigma_r - \varepsilon_r$ stress-strain curve computed using the critical finite element of the finite element model and the $\sigma_r - \varepsilon_r$ stress-strain curve obtained experimentally let us conclude that the way we used for determining the material properties is validated for both kinds of aluminum alloys involved in this research.

Moreover, in future research the input parameters determined for FEA (Young's modulus E, the true stress σ_r and true strain ε_r value pairs to determine the material behavior in the plastic range) in the case of the EN AW–6060 aluminum alloy in T4 or T6 heat treatment condition can also be used to determine the material properties for a FEA concerning any mechanical structure and/or structural element made of such aluminum alloy.

Acknowledgement. The authors hereby acknowledge the structural fund project PRO-DD (POS-CCE, O.2.2.1., ID 123, SMIS 2637, ctr. No 11/2009) and the Transylvania University of Braşov for providing the infrastructure used in this work.

References

1. Chen, R., Xu, Q., Guo, H., Xia, Z., Wu, Q. and Liu, B.: Correlation of solidification microstructure refining scale, Mg composition and heat treatment conditions with mechanical properties in Al-7Si-Mg cast aluminum alloys. *Materials Science and Engineering A*, **685**, (2017), 391-402.
2. Jung, J. G., Lee, J. M., Cho, Y. H. and Yoon, W. H.: Combined effects of ultrasonic melt treatment, Si addition and solution treatment on the microstructure and tensile properties of multicomponent AlSi alloys. *Journal of Alloys and Compounds*, **693**, (2017), 201-210.
3. Peng, Y., Li, S., Deng, Y., Zhou, H., Xu, G. and Yin, Z.: Synergetic effects of Sc and Zr microalloying and heat treatment on mechanical properties and exfoliation corrosion behavior of Al-Mg-Mn alloys. *Materials Science and Engineering: A*, **666**, (2016), 61-71.
4. Lee, Y. S., Cha, J. H., Kim, S. H., Lim, C. Y. and Kim, H.W.: Effect of prehomogenization deformation treatment on the workability and mechanical properties of AlMg5Si2Mn alloy. *Materials Science and Engineering: A*, **685**, (2017), 244-252.

5. Aboulkhair, N. T., Maskery, I., Tuck, C., Ashcroft, I. and Everitt, N. M.: Improving the fatigue behaviour of a selectively laser melted aluminum alloy: Influence of heat treatment and surface quality. *Materials & Design*, **104**, (2016), 174-182.
6. Ding, J. K, Wang, D. P., Wang, Y. and Du, H.: Effect of post weld heat treatment on properties of variable polarity TIG welded AA2219 aluminum alloy joints. *Transactions of Nonferrous Metals Society of China*, **24**(5), (2014), 1307-1316.
7. Zhong, H., Rometsch, P. and Estrin, Y.: Effect of alloy composition and heat treatment on mechanical performance of 6xxx aluminum alloys. *Transactions of Nonferrous Metals Society of China*, **24**(7), (2014), 2174-2178.
8. Li, Q., Li, F., Xia, T., Lan, Y., Jian, Y. and Tao, F.: Effects of in-situ y-Al2O3 particles and heat treatment on the microstructure and mechanical properties of A356 aluminum alloy. *Journal of Alloys and Compounds*, **627**, (2015), 352-358.
9. Lu, Y., Wang, J., Li, X., Chen, Y., Zhou, D., Zhou , G. and Xu, W.: Effect of pre-deformation on the microstructures and properties of 2219 aluminum alloy during aging treatment. *Journal of Alloys and Compounds*, **699**, (2017), 1140-1145.
10. Ashrafizadeh, S. M., Eivani, A. R., Jafarian, H. R. and Zhou, J.: Improvement of mechanical properties of AA6063 aluminum alloy after equal channel angular pressing by applying a two-stage solution treatment. *Materials Science and Engineering: A*, **687**, (2017), 54-62.
11. Niklas, A., Orden, S., Bakedano, A., Da Silva, M., Nogués, E. and Fernández-Calvo, A. I.: Effect of solution heat treatment on gas porosity and mechanical properties in a die cast step test part manufactured with a new AlSi10MnMg(Fe) secondary alloy. *Materials Science and Engineering: A*, **667**, (2016), 376-382.
12. Akhil, K.T., Arul, S. and Sellamuthu, R.: The effect of heat treatment and aging process on microstructure and mechanical properties of A356 aluminum alloy sections in casting. *Procedia Engineering*, **97**, (2014), 1676-1682.
13. Yang, H., Ji, S. and Fan, Z.: Effect of heat treatment and Fe content on the microstructure and mechanical properties of die-cast Al–Si–Cu alloys. *Materials & Design*, **85**, (2015), 823-832.
14. Maisonnette, D., Suery, M., Nelias, D., Chaudet, P. and Epicier T.: Effects of heat treatments on the microstructure and mechanical properties of a 6061 aluminum alloy. *Materials Science and Engineering: A*, **528**(6), (2011), 2718-2724.
15. Shin, J., Kim, T., Kim D. E., Kim, D. and Kim, K.: Castability and mechanical properties of new 7xxx aluminum alloys for automotive chassis/body applications. *Journal of Alloys and Compounds*, **698**, (2017), 577-590.
16. Geetha, B. and Ganesan, K.: The effects of aging temperature and time on mechanical properties of A356 aluminum cast alloy with red mud addition and treated by T6 heat treatment. *Materials Today: Proceedings*, **2**(4–5), (2015), 1200-1209.
17. Maisonnette, D., Bardel, D., Robin, V., Nelias, D. and Suery, M.: Mechanical behavior at high temperature as induced during welding of a 6xxx series aluminum alloy. *International Journal of Pressure Vessels and Piping*, **149**, (2017), 55-65.
18. Rometsch, P. A., Zhang, Y. and Knight, S.: Heat treatment of 7xxx series aluminum alloys—Some recent developments. *Transactions of Nonferrous Metals Society of China*, **24**(7), (2014), 2003-2017.

19. Robinson, J. S. and Redington, W.: The influence of alloy composition on residual stresses in heat treated aluminum alloys. *Materials Characterization*, **105**, (2015), 47-55.

20. BS EN 755-2: 1997. Aluminium and aluminum alloys – Extruded rod/bar, tube and profiles. Part 2: Mechanical properties. 1997.

21. BS EN 515:1993. Aluminium and aluminum alloys. Wrought products. Temper designations. Standard by British-Adopted European Standard, 10/15/1993.

22. Santaoja, K.: Viscous and elastic-plastic material model in the ABAQUS. *Metal laboratory. VTT Publications 144, Technical Research Centre of Finland Espoo*, 1993, pp. 3-54. ISBN 951-38-4382-3, ISSN 1235-0621.

23. Wang, B., Chen, X. H, Pan, F. S., Mao J. J. and Fang, Y.: Effects of cold rolling and heat treatment on microstructure and mechanical properties of AA 5052 aluminum alloy. *Transactions of Nonferrous Metals Society of China*, **25**(8), (2015), 2481-2489.

24. SR EN 573-3: 2010. Aluminium and aluminum alloys. Chemical composition and form of wrought products. Part 3: Chemical composition and form of products. Romanian Standard version, ASRO, 2010.

25. SR EN 573-5: 2008. Aluminium and aluminum alloys. Chemical composition and form of wrought products. Part 5: Codification of standardized wrought products. Romanian Standard version, ASRO, 2008.

26. SR EN ISO 6892-1: 2010 (or EN ISO 6892-1: 2002). Metallic materials. Tensile testing. Part 1: Method of test at room temperature.

27. http://www.euralliage.com/6060.htm